Analysis of the Influence of Viscosity and Thermal Conductivity on Heat Transfer by Al_2O_3-Water Nanofluid

Houda Jalali[1,*] and Hassan Abbassi[1]

Abstract: The addition of nanoparticles into liquid, even at low concentrations, leads to an increase in both, dynamic viscosity and thermal conductivity. Furthermore, the increase in temperature causes an increase in thermal conductivity and a decrease in the nanofluid viscosity. In this context, a numerical investigation of the competition between viscosity and thermal conductivity about their effects on heat transfer by Al_2O_3-water nanofluid was conducted. A numerical study of heat transfer in a square cavity, filled with Al_2O_3-water nanofluid and heated from the left side, was presented in this paper. Continuity, momentum, and thermal energy equations are solved by the finite volume method. Regarding the pressure-velocity coupling, the SIMPLER algorithm was used. The working conditions, allowing the increase of heat transfer, are established. In addition, two correlations for viscosity and thermal conductivity of Al_2O_3-water nanofluid as functions of the concentration and diameter size based on experimental measurement are proposed. These correlations were more precisely compared to those given by the theoretical models. Moreover, other models for viscosity and conductivity depending on temperature are used and discussed. The results reveal that heat transfer by Al_2O_3-water nanofluid is enhanced only when the temperature exceeds 40°C and the diameter size does not exceed a certain limit of the order of 45-50 nm depending on temperature.

Keywords: Heat transfer, nanofluid, viscosity, thermal conductivity.

Nomenclature

Cp	specific heat at constant pressure ($J.kg^{-1}.K^{-1}$)
d_f	the equivalent diameter of fluid molecule
d_p	(m)
g	nanoparticles diameter (m)
k	gravitational acceleration ($m.s^{-2}$)
$k_r=k_{nf}/k_f$	thermal conductivity ($W.m^{-1}.K^{-1}$)
L	relative thermal conductivity
Nu	length of the cavity (m)
P	space averaged Nusselt number
$Pr = \nu_f / \alpha_f$	dimensionless pressure

[1] Unit of Computational Fluid Dynamics and Transfer Phenomena, National Engineering School of Sfax (ENIS), University of Sfax, Sfax, Tunisia.
[*] Corresponding Author: Houda Jalali. Email: houda-jlali@hotmail.fr.
Received: 11 December 2018; Accepted: 30 June 2019.

$Ra = g\beta_f L^3 (T_h - T_c) \,/\, \nu_f \alpha_f$	Prandtl number
T	Rayleigh number
U, V	temperature (K)
X, Y	dimensionless velocity components
	dimensionless coordinates
Greek symbols	dimensionless temperature
$\theta = (T - T_c) \,/\, (T_h - T_c)$	density ($kg.m^{-3}$)
ρ	dynamic viscosity of the fluid ($kg.m^{-1}.s^{-1}$)
μ	thermal diffusivity ($m^2.s^{-1}$)
$\alpha = k \,/\, \rho C_p$	thermal expansion coefficient (K^{-1})
β	kinematic viscosity of the fluid ($m^2.s^{-1}$)
$\nu = \mu/\rho$	solid volume fraction
ϕ	
Subscripts	cold
c	fluid
f	hot
h	nanofluid
nf	solid
s	

1 Introduction

Nanofluid is a suspension of metallic nanoparticles such as Cu, CuO, Al_2O_3 or TiO_2 dispersed within a base liquid like water, oil and ethylene glycol. In the last few years, researches pertaining to convective heat transfer, using nanofluid, have proliferated. Nanofluids possess numerous significant applications in scientific engineering such as solar collector, electronic components cooling and heat exchangers. In fact, several numerical and experimental studies concerned with the analysis of the heat transfer behavior of nanofluids in cavities have gained momentum.

Lai et al. [Lai and Yang (2011)] simulated natural convection heat transfer of Al_2O_3-water nanofluid in a square enclosure. They used the lattice Boltzmann method (LBM) for simulations. They found that the increase of the nanoparticle volume fraction leads to an increase on Nusselt numbers. They also noted that theoretical models under-estimate the nanofluid viscosity. Mejri et al. [Mejri, Mahmoudi, Abbassi et al. (2014)] studied the Magneto Hydro Dynamics (MHD) natural convection heat transfer in square cavity filled with different types of nanofluid. They reported that the incorporation of the nanoparticles into fluid enhances heat transfer. Bouchoucha et al. [Bouchoucha and Bessaïh (2015)] analyzed numerically a two-dimensional laminar natural convection in a square cavity filled with nanofluids. Their results indicated that heat transfer is enhanced when the concentration increase. Boualit et al. [Boualit, Zeraibi, Chergui et al. (2016)] performed a numerical study of natural convection in a square enclosure filled with Cu-water nanofluid for different Rayleigh numbers. Results display an increase in the Nusselt number according to the volume fraction for all Rayleigh numbers and various diameters sizes. Kolsi [Kolsi (2016)] conducted a numerical study of natural convection, using Al_2O_3-

water nanofluid within an enclosure. This enclosure is equipped with a conductive baffle attached to the top adiabatic wall. Simulations show that, for $Ra=10^6$, when the concentration of nanofluid shifts from 0 to 0.2, the Nusselt number increases to reach 76.2%. Salari et al. [Salari, Malekshah and Malekshah (2018)] numerically examined the effect of nanoparticles on heat transfer in natural convection in a rectangular enclosure, using Al_2O_3-water nanofluids for different Rayleigh numbers ranging from 10^3 to 10^6 and for concentrations varying from 0 to 0.2. They found that heat transfer is enhanced with Rayleigh number and with the solid volume fraction.

With reference to the afore-mentioned bibliography, most studies reported that the addition of nanoparticles in basic fluid enhances heat transfer, even at room temperature. The majority of these works used theoretical models of viscosity and thermal conductivity, namely Brinkman [Brinkman (1952)] and Maxwell [Maxwell (1904)] models, respectively. Currently, many experimental researches existing in the literature have investigated the dynamic viscosity and thermal conductivity of nanofluids. It can be noted that the theoretical models underestimates viscosity, especially at high concentrations of nanoparticles. On the other hand, the Maxwell model pertaining to the thermal conductivity needs to incorporate the parameters of the diameter size (dp) and the temperature (T).

In the literature, several researchers Nguyen et al. [Nguyen, Desgranges, Roy et al. (2007); Pastoriza-Gallego, Casanova, Legido et al. (2011); Kulkarni, Das and Vajjha (2009); Kumar, Sawhney, Sharma et al. (2016)] experimentally measured the effect of concentration, temperature and diameter size on the viscosity of nanofluids. Results reveal that the increase of temperature leads to a decrease in nanofluid viscosity. Ahangarpour et al. [Ahangarpour and Farbod (2016)] realized an experimental study regarding the effect of temperature on thermal conductivity of CNTs-EG nanofluid. The experimental data show that at all measured temperatures, the use of the carbon nanotubes (CNTs) into ethylene glycol (EG) enhance the thermal conductivity of CNTs-EG nanofluids.

The present paper aims to study the performance of Al_2O_3-water nanofluid in square cavity heated from one vertical wall. The effect of various operating parameters such as solid volume fraction (ϕ), Rayleigh number (Ra), temperature (T), diameter size (dp), viscosity and thermal conductivity, on heat transfer enhancement is investigated. For this reason, models for viscosity and thermal conductivity, based on experimental data of Al_2O_3-water nanofluid valid at ambient temperature, are developed. Other models based on experimental measurements combining effects of temperature, concentration and diameter size are also used to evaluate heat transfer by Al_2O_3-water nanofluid.

2 Nanofluid properties

Tab. 1 presents the thermophysical properties of base fluid and Al_2O_3 nanoparticles at ambient temperature.

Table 1: Thermophysical properties of base fluid and Al_2O_3 nanoparticles

Property	k $W.m^{-1}.K^{-1}$)	ρ $(kg.m^{-3})$	C_p $(J.kg^{-1}.K^{-1})$	β (K^{-1})
Base fluid (Water)	0.613	997.1	4179	21×10^{-5}
Al_2O_3 nanoparticle	40	3970	765	0.85×10^{-5}

The density of nanofluid is calculated from the following relation:

$$\rho_{nf} = (1-\phi)\rho_f + \phi\rho_s \tag{1}$$

where ϕ refers to the solid volume fraction of nanofluid, the subscripts *nf, f* and *s* stand for the nanofluid, the base fluid and the solid particles respectively.

The specific heat is obtained by Abu-Nada et al. [Abu-Nada, Masoud, Oztop et al. (2010)].

$$(\rho Cp)_{nf} = (1-\phi)(\rho Cp)_f + \phi(\rho Cp)_s \tag{2}$$

The thermal expansion coefficient is assessed by Ghasemi et al. [Ghasemi and Aminossadati (2009)] defined by:

$$(\rho\beta)_{nf} = (1-\phi)(\rho\beta)_f + \phi(\rho\beta)_s \tag{3}$$

Relations (2) and (3) are inspired from Eq. (1).

Brinkman [Brinkman (1952)] and Batchelor [Batchelor (1977)] models of viscosity nanofluid as function of volume fraction are expressed as follows:

$$\mu_{nf} = \frac{\mu_f}{(1-\phi)^{2.5}} \tag{4}$$

$$\mu_{nf} = (1 + 2.5\phi + 6.2\phi^2)\mu_f \tag{5}$$

From experimental data found in the literature of Nguyen et al. [Nguyen, Desgranges, Roy et al. (2007); Pak and Cho (1998); Wang, Xu and Choi (1999)], it appears that the dynamic viscosity of Al_2O_3-water nanofluid is largely underestimated by theoretical models, especially at high solid volume fraction. Regarding the experience of Nguyen et al. [Nguyen, Desgranges, Roy et al. (2007)] and at 5% nanofluid concentration, the dynamic viscosity of Al_2O_3-water nanofluid is equal to 0.002 *Pa.s*. On the other hand, for the same concentration, Brinkman model gives a viscosity of only 0.0011 *Pa.s*, the deviation of the model to experiment is of the order of 45%. This strong divergence between experimental and theoretical values raises doubts about the finding that the additions of nanoparticles into basic fluid lead to an increase in heat transfer. This was our main motivation to find new more precise models, taking into account the effects of concentration and diameter size. Using the smoothing of measurements of Nguyen et al. [Nguyen, Desgranges, Roy et al. (2007); Pak and Cho (1998); Wang, Xu and Choi (1999)] by minimum mean square error method and taking into consideration the Lagrangian polynomial interpolation allows us to the following model pertaining to viscosity as a function of concentration ϕ and the diameter size d_p:

$$\frac{\mu_{nf}}{\mu_f} = \left[-243.17\left(\frac{d_f}{d_p}\right)^2 + 11.83\frac{d_f}{d_p} - 0.0853\right]\phi^2 + \left[1878.4\left(\frac{d_f}{d_p}\right)^2 - 55.26\frac{d_f}{d_p} + 0.4027\right]\phi + 1 \quad (6)$$

$0\% \leq \phi \leq 5\%, 13\ nm \leq dp \leq 36\ nm$

where d_p and d_f are, respectively, the diameters of the spherical nanoparticles Al_2O_3 and the base fluid molecule.

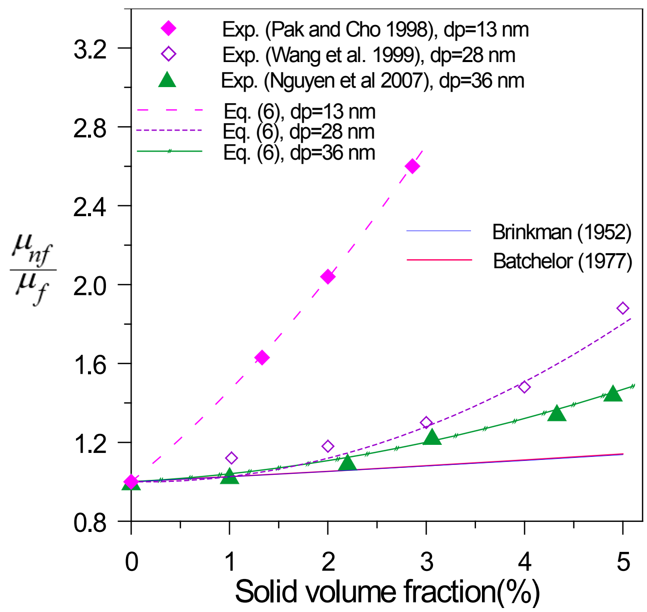

Figure 1: Comparison of the new model of viscosity Al_2O_3-water model to experiments data: Curves corresponding to theoretical models Batchelor [Batchelor (1977)] and Brinkman [Brinkman (1952)] are confounded for this scale of μ_{nf}/μ_f

Fig. 1 reveals that our new model given by Eq. (6) follows correctly the viscosity. The maximum deviation of the model with experimental data is 3.41%. Based on this figure, the classical models of Brinkman [Brinkman (1952)] and Batchelor [Batchelor (1977)] (curves are confounded in Fig. 1) under-estimate the viscosity, notably at high solid volume fraction.

In the same way as the viscosity, new correlation of Al_2O_3-water nanofluid thermal conductivity as a function of solid volume fraction and diameters is presented in this study. Experimental data, available in the literature reported by Masuda et al. [Masuda, Ebata, Teramae et al. (1993); Eastman, Choi, Li et al. (1997); Das, Li, Thiesen et al. (2003)] are used to derive this correlation.

$$\frac{k_{nf}}{k_f} = \left[-0.0266\left(\frac{d_p}{d_f}\right)^2 + 3.8909\left(\frac{d_p}{d_f}\right) - 148.5075\right]\phi^2 + \left[-0.0022\left(\frac{d_p}{d_f}\right)^2 + 0.2062\left(\frac{d_p}{d_f}\right) + 4.8860\right]\phi + 1 \quad (7)$$

$$0\% \leq \phi \leq 5\%, 13\ nm \leq dp \leq 38.4\ nm$$

Fig. 2 indicates that our proposed model Eq. (7) predicts acceptably the thermal conductivity for Al_2O_3-water nanofluid. The maximum deviation of the model with experimental data is of the order of 2.3%.

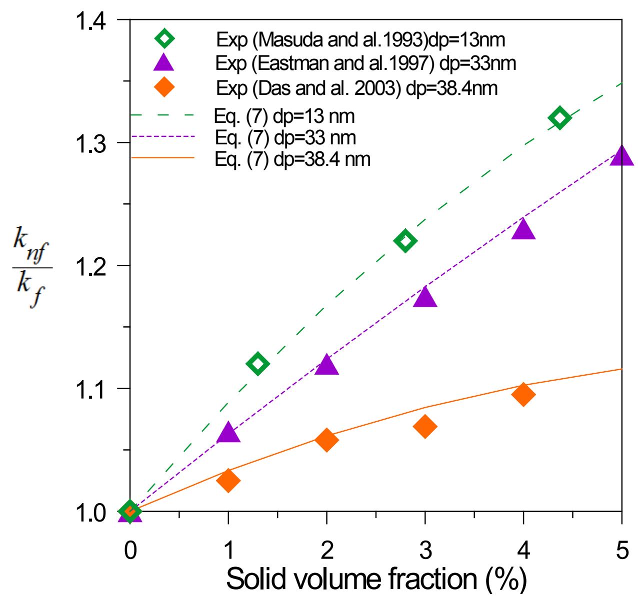

Figure 2: Comparison of the proposed model with those experiments for Al_2O_3-water thermal conductivity

From Eqs. (6) and (7), a concentration of 3% and a diameter size of 13 nm lead to an augmentation of 25% and 170% in thermal conductivity and viscosity respectively. This information makes us in serious doubt concerning the findings in many last publications in which authors concluded that adding nanoparticles increases the heat transfer despite this amazing increase in viscosity [Khanafer, Vafai and Lightstone (2003); Mejri, Mahmoudi, Abbassi et al. (2014); Oztop and Abu-Nada (2008)]. In the following, natural convection flow in a square cavity filled by nanofluid is considered to verify if the addition of solid particle into basic liquid enhances heat transfer and to study the contradictory roles played by viscosity and thermal conductivity.

3 Numerical modelling

In the case of natural convection, the present numerical study deals with the effects of adding nanoparticles Al_2O_3 into pure water on heat transfer in a square cavity heated from vertical side as presented in Fig. 3. The flow is supposed to be laminar and bi-dimensional. The Al_2O_3-water nanofluid is assumed to be Newtonian and incompressible.

Moreover, the nanofluid is considered as a single phase fluid with thermal equilibrium between the pure water and the nanosolid particles suspended in it.

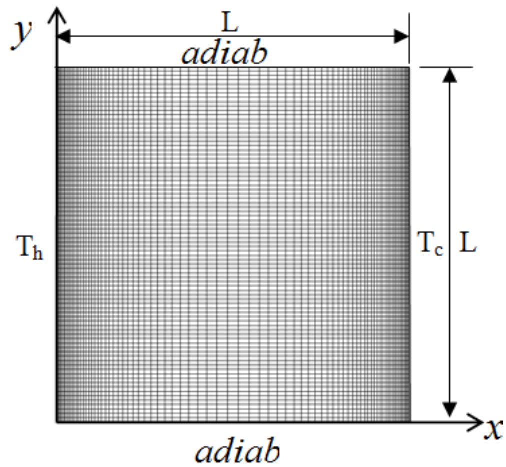

Figure 3: Meshing of the geometry and boundary conditions

The numerical solutions of fluid flow equations were presented to simulate the total heat transferred from the hot wall to the flow.

The governing equations for the nanofluid flow are the continuity, momentum and thermal energy equations:

$$\frac{\partial U}{\partial X} + \frac{\partial V}{\partial Y} = 0 \tag{8}$$

$$U\frac{\partial U}{\partial X} + V\frac{\partial U}{\partial Y} = -\frac{\partial P}{\partial X} + \frac{\mu_{nf}}{\rho_{nf}\alpha_f}\left(\frac{\partial^2 U}{\partial X^2} + \frac{\partial^2 U}{\partial Y^2}\right) \tag{9}$$

$$U\frac{\partial V}{\partial X} + V\frac{\partial V}{\partial Y} = -\frac{\partial P}{\partial Y} + \frac{\mu_{nf}}{\rho_{nf}\alpha_f}\left(\frac{\partial^2 V}{\partial X^2} + \frac{\partial^2 V}{\partial Y^2}\right) + \frac{(\rho\beta)_{nf}}{\rho_{nf}\beta_f} RaPr\theta \tag{10}$$

$$U\frac{\partial \theta}{\partial X} + V\frac{\partial \theta}{\partial Y} = \frac{\alpha_{nf}}{\alpha_f}\left(\frac{\partial^2 \theta}{\partial X^2} + \frac{\partial^2 \theta}{\partial Y^2}\right) \tag{11}$$

The dimensionless form of governing equations can be obtained using the characteristic length L of the square cavity; the specific velocity $\frac{\alpha_f}{L}$ and the dimensionless temperature are defined as $\theta = (T - T_c)/(T_h - T_c)$.

where α_f is the thermal diffusivity of the fluid.

Prandtl and Rayleigh numbers in Eq. (10) designed by *Pr* and *Ra* respectively are defined by: $= \frac{\nu_f}{\alpha_f}$; $Ra = \frac{g\beta_f L^3 (T_h - T_c)}{\nu_f \alpha_f}$.

The dimensionless boundary conditions considered in this study are:

- At the horizontal walls: $U = V = 0, \frac{\partial \theta}{\partial Y} = 0$
- X=0, 0≤Y≤1: $U = V = 0, \theta = 1$

- X=1, 0≤Y≤1: $U = V = \theta = 0$

The averaged Nusselt number is defined as:

$$Nu = -\frac{k_{nf}}{k_f}\int_0^1 \frac{\partial\theta}{\partial X}\Big)_{X=0} dY \tag{12}$$

4 Grid sensitivity test and code validation

The grid sensitivity tests of the present results has been related to pure water at Ra=10^6. The Prandtl number is fixed at 6.83 using five non-uniform grids. Tab. 2 presents the Nusselt number calculated at the hot wall of the cavity for different grids. As shown in this table, a grid of 81×81 yields a good compromise between precision and calculation time and it is sufficient to carry out a numerical study of this flow.

Table 2: Grid sensitivity tests

Grid	**51×51**	**61×61**	**71×71**	**81×81**	**91×91**
Nusselt number	9.3074	9.2885	9.2757	9.2717	9.2686

In order to verify the precision of the present study, a validation was conducted for different Rayleigh numbers, varying from 10^3 to 10^6. Tab. 3 compares *Nu* of the present simulations to the results of Lai et al. [Lai and Yang (2011)] and Kahveci [Kahveci (2010)]. The maximum difference between the results for pure water and 1% solid volume fraction of Al_2O_3-water is less than 1.08% and 3.2%, respectively. From validation, a good agreement can be observed between the results of the present study and those of Lai et al. [Lai and Yang (2011)] and Kahveci [Kahveci (2010)].

Table 3: Code Validation

		***Ra*=10^3**	***Ra*=10^4**	***Ra*=10^5**	***Ra*=10^6**
Pure water	**Current study**	**1.1218**	**2.2856**	**4.7388**	**9.2717**
	[Lai and Yang (2011)]	1.128	2.286	4.729	9.173
	[Kahveci (2010)]	---	2.274	4.722	9.230
$\boldsymbol{\phi = 1\%}$	**Current study**	**1.1218**	**2.3123**	**4.8020**	**9.4349**
	[Lai and Yang (2011)]	1.1600	2.3518	4.8642	9.4329

5 Computations under the hypothesis of room temperature

A numerical study was performed to investigate the effects of viscosity, thermal conductivity, solid volume fraction, diameter size, Rayleigh number and temperature on heat transfer in a square cavity filled with Al_2O_3-water nanofluid. In this section, the temperature is fixed at room temperature.

In Fig. 4 the impact of the solid volume fraction ϕ of Al_2O_3 on the Nusselt numbers, using our models for dynamic viscosity Eq. (6) and thermal conductivity Eq. (7) in comparison with the results given by the model of Brinkman Eq. (4), is studied for different Rayleigh numbers. As noted in this figure, our models of viscosity and thermal conductivity lead to the decrease in Nusselt number, when the solid volume fraction ϕ increases. This behavior is pronounced when *Ra* augments. Thus, this result has attracted our attention due to its surprising aspect. In fact, in the majority of the literature, adding the nanoparticles in basic fluid leads permanently to an increase in heat transfer. The obvious question, at this stage, is why our models lead to the decrease in *Nu*, while the Brinkman model of dynamic viscosity leads to an increase in Nusselt number. It is noteworthy that the addition of nanosuspensions in fluid plays a double role. On the one hand, it increases the thermal conductivity of the nanofluid, and subsequently causing an increase of heat transfer, especially by conduction from the hot wall of the cavity to the flow. On the other hand, it results in an increase of nanofluid, thus slowing the flow motion which gives rise to a decrease in heat transfer by convection inside the cavity.

The purpose of this work is to evince which factor plays the significant role, the increase in viscosity or in thermal conductivity after adding the nanoparticles into fluid. From Fig. 4, it is clear that at 5% solid volume fraction and size particles d_p=17 nm, the enhancement of the nanofluid thermal conductivity is about 41.36%, while the increase of viscosity is of the order of 206.7% for our model and 13.67% only for Brinkman model. It seems worth pointing out that our model pertaining to viscosity of nanofluid derived from experimental measurements is more credible than Brinkman model, which is based on theoretical estimations. Now the behaviour of *Nu* as a function of ϕ presented in Fig. 4 can be explained; the increase in nanofluid viscosity after the addition of nanosuspensions prevails over the increase in thermal conductivity. As a consequence, enhancement of heat transfer from the hot wall by conduction is not sufficient to offset the decline in heat transfer by convection after the braking of the flow motion under viscosity effects.

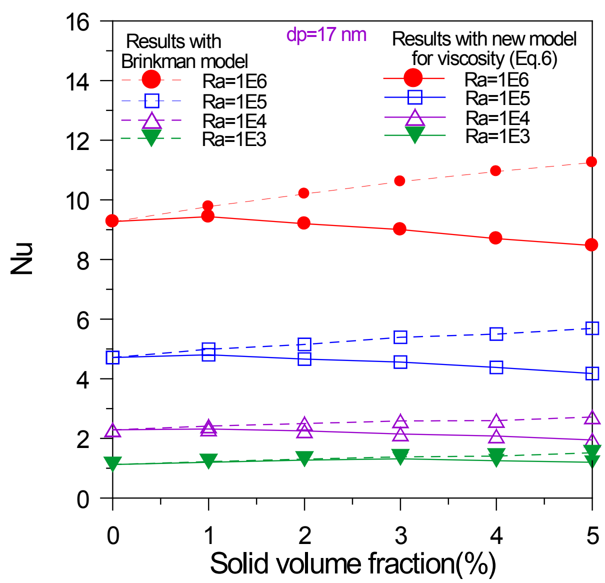

Figure 4: Effect of the solid volume fraction of Al_2O_3-water nanofluid with different Rayleigh numbers on the Nusselt number via a comparison between our models (continuous curves) and Brinkman model for viscosity (discontinuous curves)

Fig. 5 shows the flow structure in the cavity for different Rayleigh numbers in the case of pure water and ϕ=5% for concentration of Al_2O_3-water nanofluid. It can be seen that, at

Ra=10^4, the flow is characterized by the presence of unicellular vortex within the square cavity. When the nanofluid receives heat from the hot wall it becomes lighter and the buoyancy forces make it in upward flow. On the other hand, next to the cold wall, the nanofluid becomes heavier and descends along this wall. The increase in the number of Rayleigh leads to an intensification of the boundary layer near the active walls. At a high Rayleigh number (*Ra*=10^6), the flow structure is characterized by the existence of two small cells in the vicinity of the active walls, enveloped by a single large cell that occupies the entire cavity.

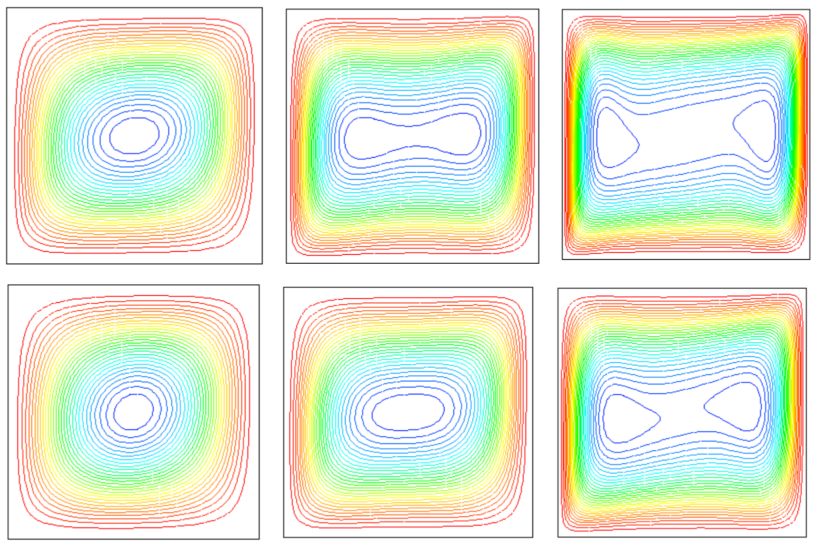

(a): ϕ=0%

(b): ϕ=5%

Ra=10^4 *Ra*=10^5 *Ra*=10^6

Figure 5: Streamlines for the cavity filled with Al_2O_3-water nanofluid at *Ra*=10^4, 10^5 and 10^6; (a): ϕ=0%, (b): ϕ=5%

6 Computations for various temperatures

As discussed above, at room temperature, the addition of solid particle in liquid decreases heat transfer. The system becomes useful in insulation system, while useless for systems where thermal exchange is needed. From a molecular viewpoint, when the temperature of the fluid increases, the intermolecular distance becomes larger, leading to the decrease of viscosity. Besides, the agitation in microscopic scale becomes stronger, causing an increase in thermal conductivity. Hence, studying the effects of temperature on thermal conductivity, viscosity and heat transfer, in order to to determine the conditions that allow an increase in heat transfer is required. Subsequently, models of viscosity and thermal conductivity, expressed as functions of temperature, are required. These models are developed by Khanafer et al. [Khanafer and Vafai (2011)] and based on the experimental measurements of Al_2O_3-water nanofluid.

$$k_r = 0.9843 + 0.398\phi^{0.7383}\left(\frac{1}{d_p}\right)^{0.2246}\left(\frac{\mu_{nf}}{\mu_f}\right)^{0.0235} - 3.9517\frac{\phi}{T} + 34.034\frac{\phi^2}{T^3} + 32.509\frac{\phi}{T^2} \tag{14}$$

$$\mu_f(T) = 2.414\,10^{-5}\,10^{247.8/(T-140)} \tag{15}$$

$$\mu_{nf} = -0.4491 + \frac{28.837}{T} + 0.5740\phi - 0.1634\phi^2 + 23.053\frac{\phi^2}{T^2} + 0.0132\phi^3 - 2354.734\frac{\phi}{T^3} + 23.498\frac{\phi^2}{d_p^2} - 3.0185\frac{\phi^3}{d_p^2} \tag{16}$$

The variation of the relative thermal conductivity k_r of the Al_2O_3-water nanofluids as a function of temperature is displayed in Fig. 6. Obviously, temperature has a significant impact on the variation of the relative thermal conductivity. When temperature increases, kr increases considerably. Likewise, at ϕ=5% and as temperature shifts from 20°C to 70°C, k_r undergoes a growth of the order of 20.65%. A total increase of 26.16% in the thermal conductivity ratio is recorded, when shifting from ϕ=1% and T=20°C to ϕ=5% and T=70°C.

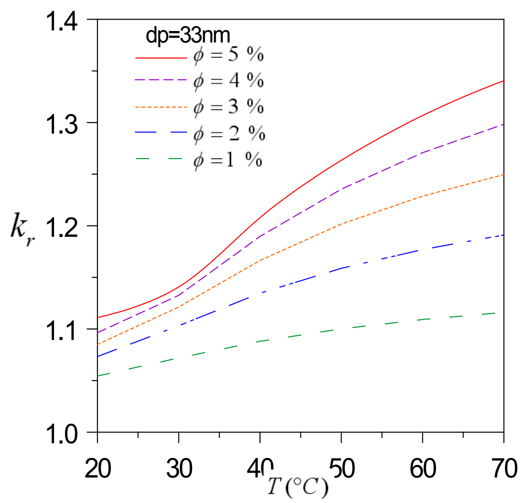

Figure 6: Variation of the relative thermal conductivity Al_2O_3-water *vs.* temperature

Fig. 7 represents the influence of the temperature for different solid volume fractions on the nanofluid viscosity. This figure indicates that the increase of temperature leads to a decrease of viscosity. Taking as example the case of 5% solid volume fraction, viscosity is found to be reduced by 57.59% once the temperature shifts from 20°C to 70°C.

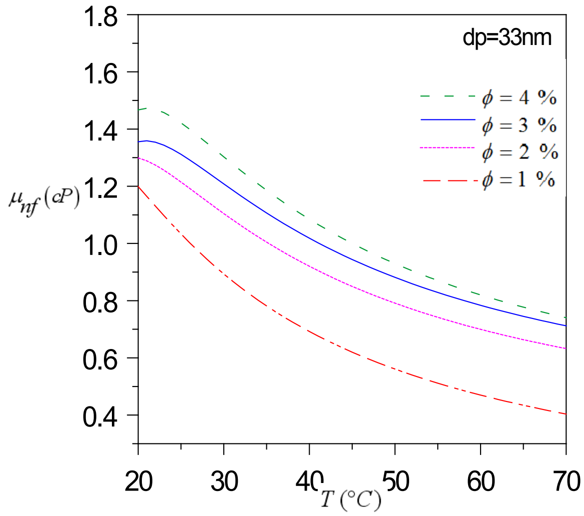

Figure 7: Variation of the viscosity *vs.* temperature

The behavior of the decrease on the viscosity and of the increase on the thermal conductivity with the elevation of the temperature seems promising with respect to the improvement of heat transfer by Al_2O_3-water nanofluid. For this purpose, the Nusselt number characterizing heat transfer is computed versus the temperature for different concentrations. Results are shown in Fig. 8. It is noted that for all concentrations, increasing the mean temperature of the nanofluid leads to the increase of the Nusselt number. Taking as an illustration the case of 5% of concentration, and in the temperature range 20°C to 70°C, the enhancement of the Nusselt number is of the order of 15.34%. This figure exhibits the existence of two intervals temperature; 20°C≤T≤40°C and 40°C≤ T≤70°C. For the first interval, the Nusselt number decreases with increasing the concentrations, i.e., the dispersion of solid nanoparticles into fluid leads to a decrease in heat transfer; in this case, the growth in viscosity is prevailing over the augmentation of the thermal conductivity, even when temperature increases up to 40°C. Regarding the second temperature interval, it can be seen that the Nusselt number increases as the concentration increases. This tendency indicates that the addition of nanoparticles Al_2O_3 into pure water causes an increase in heat transfer. Moreover, the effect of increasing thermal conductivity prevails over the increase in nanofluid viscosity. The increase in temperature has also significant effects on flow speed, as well as heat transfer.

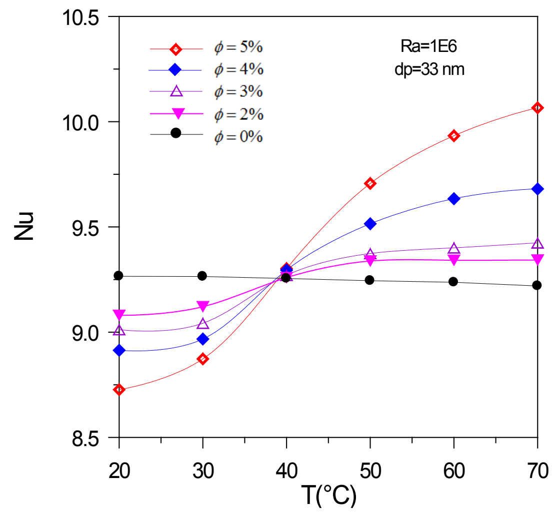

Figure 8: Effect of temperature on Nusselt number for different volume fractions of Al_2O_3

Fig. 9 shows the dimensionless vertical velocity component profile at the midplane cavity (y=0.5) at Ra=10^6 and ϕ=5% with various temperatures. From this figure, it appears that the dimensionless vertical velocity increases near the heated side of the square cavity, owing to the thermal buoyancy effects, and diminishes near the cold side of the cavity. As discussed above, the effective viscosity decreases considerably with increasing temperature, consequently, friction forces are reduced, the flow becomes freer, and velocities are as important as temperature increases. Thus, this is a favorable situation to enhance heat transfer.

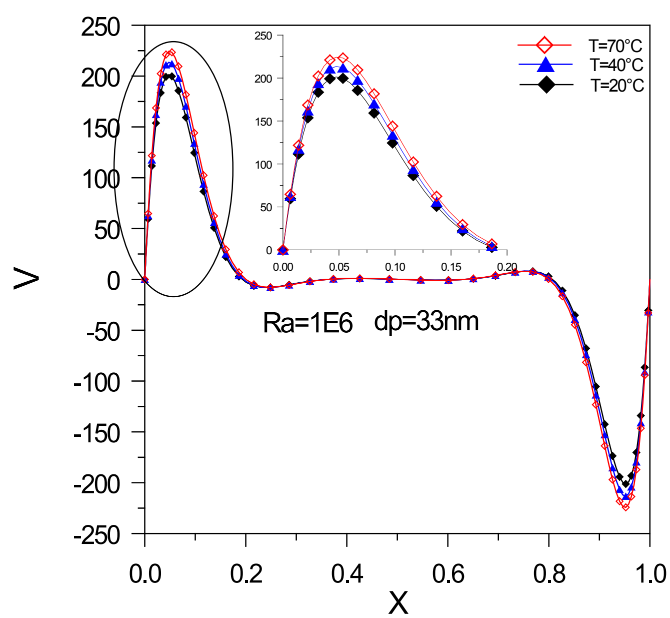

Figure 9: Velocity profile at midplane cavity (y=0.5)

7 Effects of diameter size

Fig. 10 presents the variation of the relative viscosity Eq. (6) and the relative thermal conductivity Eq. (7) of Al_2O_3-water nanofluid versus diameter sizes of solid particles, supposed to be spherical at ϕ=4% for different temperatures. This figure indicates that viscosity and thermal conductivity decrease when d_p increases. The decrease of viscosity is more pronounced compared to thermal conductivity. At T=70°C, when the diameter size shifts from 15 nm to 50 nm, μ_r undergoes a decrease of 55.72%, whereas k_r undergoes a decrease of only 11.78%. For the diameter size greater than 55 nm, μ_r and k_r become almost constant.

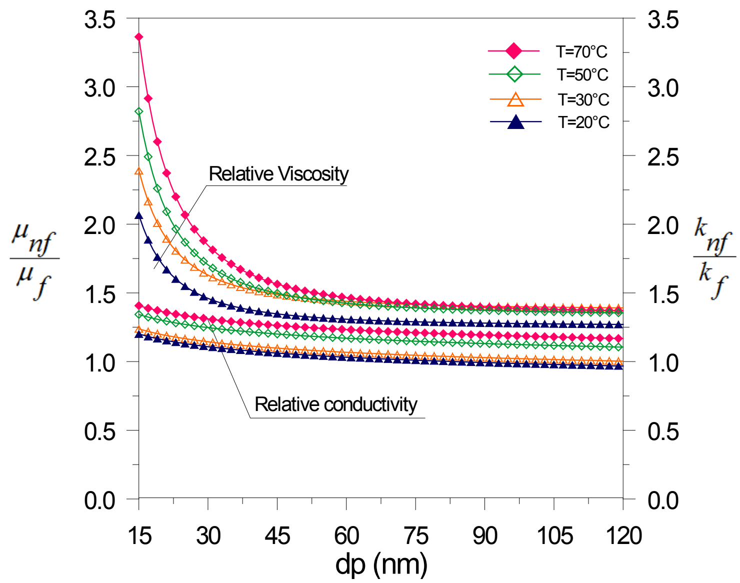

Figure 10: Effect of diameter size in relative viscosity and relative thermal conductivity of Al_2O_3-water nanofluid for different temperatures

Fig. 11 represents the influence of the nanoparticle diameter of Al_2O_3 on the average Nusselt number at $Ra=10^6$, ϕ=4%. As seen, for different temperatures, the behavior of *Nu* as a function of d_p is almost the same. *Nu* increases considerably with increasing d_p up to a maximum in the range of 45-50 nm. Taking as example the case of T=70°C, when d_p shifts from 15 nm to 50 nm, *Nu* undergoes an increase of 13.61%. The enhancement of the *Nu* is explained by the remarkable decrease of the viscosity, when the diameter size d_p shifts from 15 nm to 50 nm. Increasing the size of nanoparticles more than 50 nm has a negative effect on the heat transfer; *Nu* undergoes a slight decrease of 2.01%, when d_p passes from 50 nm to 120 nm.

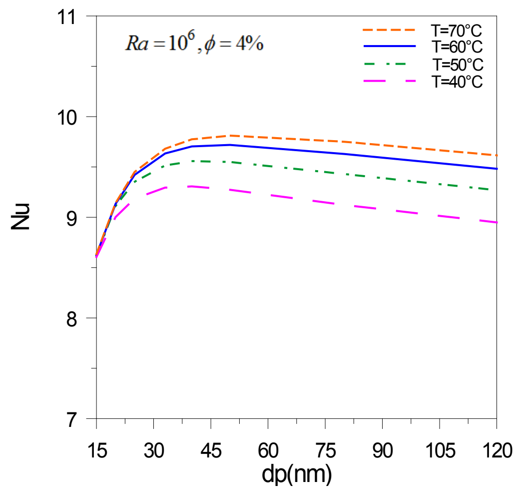

Figure 11: Influence of nanoparticle's diameter of Al_2O_3on Nusselt number

The velocity profiles at the midplane of the cavity (y=0.5) at Ra=10^6 and T=70°C for ϕ=4% is represented in Fig. 12 compared to those of pure water. In this figure, it appears that the velocity profiles of nanofluid are superior to that of water, which indicates that at high temperature, the addition of nanoparticles activates the flow dynamics. In the range of diameter sizes between 15 nm and 50 nm, the velocity profile increases as d_p increases. This behavior is explained by the significant decrease of viscosity when the diameter size varies from 15 nm to 50 nm. Beyond 50 nm, profiles remain almost unchanged. The significant variation of the attitude of the velocity profiles is ascribed to the fact that the viscosity and thermal conductivity become stable when d_p shifts from 50 nm to 120 nm.

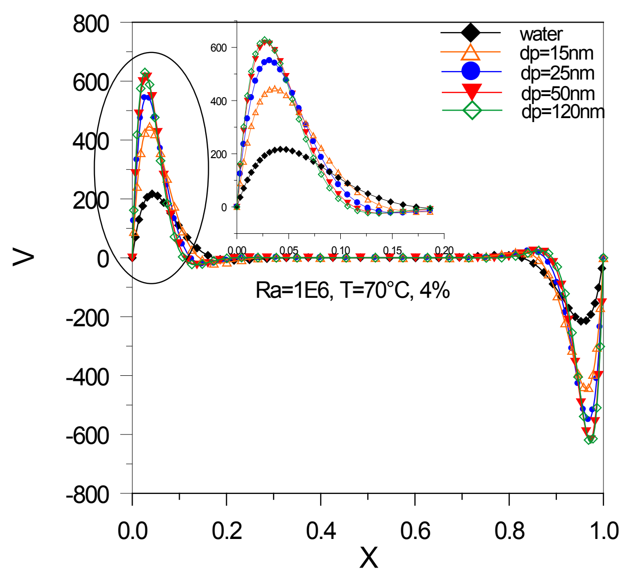

Figure 12: Velocity profile at midplane cavity at Ra=10^6 and T=70°C, for various nanoparticles sizes

8 Conclusion

In this work, the effect of adding nanosolids in pure water on viscosity, thermal conductivity and on heat transfer behavi0or, using Al_2O_3-water nanofluid in a heated square cavity was studied numerically. New models for dynamic viscosity and thermal conductivity of Al_2O_3-water nanofluid were developed based on experimental measurements. Numerical results show that solid volume fraction, temperature and diameter size yield a significant effect on dynamic viscosity and thermal conductivity of nanofluids. The contradictory effects of thermal conductivity and viscosity are discussed. At room temperature, it appears that adding Al_2O_3 nanoparticles in water leads to a strong increase in viscosity and a slight increase in thermal conductivity, thus giving rise to a decrease in heat transfer. It is found that at low temperature (T≤40°C), heat transfer decreases when Al_2O_3 nanoparticles are dispersed into water. However, at high temperature, heat transfer undergoes an increase as a function of solid volume fraction. This situation is ideal for the operating of thermal solar systems such as solar water heater, wherein the average water temperature is relatively high and can reach 80°C. Numerical simulations also indicate that heat transfer is a maximum for diameter sizes in the range of 40-50 nm, depending on operating temperature, beyond which the effect is reversed and heat transfer decreases.

References

Abu-Nada, E.; Masoud, Z.; Oztop, H. F.; Campo, A. (2010): Effect of nanofluid variable properties on natural convection in enclosures. *International Journal of Thermal Sciences*, vol. 49, pp. 479-491.

Ahangarpour, A.; Farbod, M. (2016): The noble effect of aging on the thermal conductivity of modified CNTs-ethylene glycol nanofluids. *Physics and Chemistry of Liquids*, pp. 1-7.

Batchelor, G. K. (1977): The effect of Brownian motion on the bulk stress in a suspension of spherical particles. *Journal of Fluid Mechanics*, vol. 83, pp. 97-117.

Boualit, A.; Zeraibi, N.; Chergui, T.; Lebbi, M.; Boutina, L. et al. (2017): Natural convection investigation in square cavity filled with nanofluid using dispersion model. *International Journal of Hydrogen Energy*, vol. 42, pp. 8611-8623.

Bouchoucha, A.; Bessaïh, R. (2015): Natural convection in a square cavity filled with nanofluids. *Fluid Dynamics and Materials Processing*, vol. 11, pp. 279-300.

Brinkman, H. C. (1952): The viscosity of concentrated suspensions and solution. *Journal Chemical Physics*, vol. 20, pp. 571-581.

Das, S. K.; Putra, N.; Thiesen, P.; Roetzel, W. (2003): Temperature dependence of thermal conductivity enhancement for nanofluids. *Journal of Heat Transfer*, vol. 125, pp. 567-574.

Eastman, J. A.; Choi, U. S.; Li, S.; Thompson, L. J.; Lee, S. (1997): Enhanced thermal conductivity through the development of nanofluids. *Materials Research Society*, vol. 457, pp. 3-11.

Ghasemi, B.; Aminossadati, S. M. (2009): Natural convection heat transfer in an inclined enclosure filled with a water-CuO nanofluid. *Numerical Heat Transfer Part A: Applications*, vol. 55, pp. 807-823.

Kahveci, K. (2010): Buoyancy driven heat transfer of nanofluids in a tilted enclosure. *Journal of Heat Transfer*, vol. 132, pp. 1-12.

Khanafer, K.; Vafai, K.; Lightstone, M. (2003): Buoyancy-driven heat transfer enhancement in a two-dimensional enclosure utilizing nanofluids. *International Journal Heat and Mass Transfer*, vol. 46, pp. 3639-3653.

Khanafer, K.; Vafai, K. (2011): A critical synthesis of thermophysical characteristics of nanofluids. *International Journal Heat and Mass Transfer*, vol. 54, pp. 4410-4428.

Kolsi, L. (2016): Numerical study of natural convection and entropy generation of Al_2O_3-water nanofluid within a cavity equipped with a conductive baffle. *Journal of Applied Fluid Mechanics*, vol. 9, pp. 2177-2186.

Kulkarni, D. P.; Das, D. K.; Vajjha, R. S. (2009): Application of nanofluids in heating buildings and reducing pollution. *Applied Energy*, vol. 86, pp. 2566-2573.

Kumar, M.; Sawhney, N.; Sharma, A. K.; Sharma, M. (2016): Acoustical and thermodynamical parameters of aluminium oxide nanoparticles dispersed in aqueous ethylene glycol. *Physics and Chemistry of Liquids*, vol. 55, pp. 463-472.

Lai, F. H.; Yang, Y. (2011): Lattice boltzmann simulation of natural convection heat transfer of Al_2O_3/water nanofluids in a square enclosure. *International Journal of Thermal Sciences*, vol. 50, pp. 1930-1941.

Masuda, H.; Ebata, A.; Teramae, K.; Hishinuma, N. (1993): Alteration of thermal conductivity and viscosity of liquid by dispersing ultra-fine particles, dispersion of Al_2O_3, SiO_2 and TiO_2 ultra-fine particles. *Netsu Bussei/Japan Journal of Thermophysical Properties*, vol. 7, pp. 227-233.

Maxwell, J. C. (1904): *A Treatise on Electricity and Magnetism.* Oxford University Press, Cambridge, UK.

Mejri, I.; Mahmoudi, A.; Abbassi, M. A.; Omri, A. (2014): MHD natural convection in a nanofluid-filled enclosure with non-uniform heating on both side walls. *Fluid Dynamics & Materials Processing*, vol. 10, pp. 83-114.

Nguyen, C. T.; Desgranges, F.; Roy, G.; Galanis, N.; Mare, T. et al. (2007): Temperature and particle-size dependent viscosity data for water-based nanofluids-hysteresis phenomenon. *International Journal of Heat and Fluid Flow*, vol. 28, pp. 1492-1506.

Oztop, F. H.; Abu-Nada, E. (2008): Numerical study of natural convection in partially heated rectangular enclosures filled with nanofluids. *International Journal of Heat and Fluid Flow*, vol. 29, pp. 1326-1336.

Pak, B. C.; Cho, Y. I. (1998): Hydrodynamic and heat transfer study of dispersed fluids with submicron metallic oxide particles. *Experimental Heat Transfer*, vol. 11, pp. 151-170.

Pastoriza-Gallego, M. J.; Casanova, C.; Legido, J. L.; Piñeiro, M. M. (2011): CuO in water nanofluid: influence of particle size and polydispersity on volumetric behaviour and viscosity. *Fluid Phase Equilibria*, vol. 300, pp. 188-196.

Salari, M.; Malekshah, E. H.; Malekshah, M. H. (2018): Natural convection in a rectangular enclosure filled by two immiscible fluids of air and Al_2O_3-water nanofluid heated partially from side walls. *Alexandria Engineering Journal*, vol. 57, pp. 1401-1412.

Wang, X.; Xu, X.; Choi, S. U. S. (1999): Thermal conductivity of nanoparticle-fluid mixture. *Journal of Thermophysics and Heat Transfer*, vol. 13, pp. 474-480.